Atmos. Chem. Phys. Discuss., 15, 11325–11368, 2015
www.atmos-chem-phys-discuss.net/15/11325/2015/
doi:10.5194/acpd-15-11325-2015


Atmospheric Chemistry and Physics Discussions
Open Access



# The impact of shipping emissions on air pollution in the Greater North Sea region – Part 2: Scenarios for 2030

**V. Matthias**[1], **A. Aulinger**[1], **A. Backes**[1], **J. Bieser**[1], **B. Geyer**[1], **M. Quante**[1], and **M. Zeretzke**[2]

[1]Helmholtz-Zentrum Geesthacht, Institute of Coastal Research, Max-Planck-Straße 1, 21502 Geesthacht, Germany
[2]DNV-GL, Brooktorkai 18, 20457 Hamburg, Germany

Received: 29 January 2015 – Accepted: 9 March 2015 – Published: 16 April 2015

Correspondence to: V. Matthias (volker.matthias@hzg.de)

Published by Copernicus Publications on behalf of the European Geosciences Union.

## Abstract

Scenarios for future shipping emissions in the North Sea have been developed in the framework of the Clean North Sea Shipping project. The effects of changing $NO_x$ and $SO_2$ emissions were invesigated with the chemistry transport model CMAQ for the year 2030 in the North Sea area. It has been found that, compared to today, the contribution of shipping to the $NO_2$ and $O_3$ concentrations will increase due to the expected enhanced traffic by more than 20 and 5 %, respectively, by 2030 if no regulation for further emission reductions will be implemented in the North Sea area. $PM_{2.5}$ will decrease slightly because the sulphur contents in ship fuels will be reduced as international regulations foresee. The effects differ largely between regions, seasons and date of the implementation of stricter regulations for $NO_x$ emissions from new built ships.

## 1 Introduction

Shipping is an important contributor to air pollution in coastal areas. More than 90 % of the global trade is done with ships. The total global transport work by ships (in tonne miles) has been tripled since the mid 1980s (Smith et al., 2014), corresponding to an average grow rate of 4 % $year^{-1}$, and the forecasts for the future are in the same order of magnitude (Smith et al., 2014). The North Sea is one of the areas with the highest ship densities in the world. Europe's three biggest harbours in Rotterdam, Hamburg and Antwerp are located in the North Sea region. At any time about 3000 ships are sailing in the North Sea (Aulinger et al., 2015). This steady increase in number and size of ships leads to an increasing contribution of ships to air pollution in North Sea coastal areas (Matthias et al., 2010; Hammingh et al., 2012; Jalkanen et al., 2012; Aulinger et al., 2015). Compared to other modes of transport like trucks or trains, shipping is very efficient in terms of fuel use per ton mile. However, $NO_x$, $SO_2$ and PM emissions are comparably high because of less strict regulations for the emissions of these pollutants from ships. This problem has already been recognized years ago lead-





ACPD
15, 11325–11368, 2015

ing to stricter regulations in some areas, the so called Emission Control Areas (ECAs). These regulations are the results of an agreement within the International Maritime Organization (IMO) and they are laid down in MARPOL Annex VI (International Maritime Organisation, 2008). Currently, the North and the Baltic Seas are Sulphur Emission Control Areas (SECAs), which means that the fuel burned in these areas must not contain more than 0.1 % sulphur (S) (until 31 December 2014 1.0 % S). If fuels with higher sulphur content are used, the exhaust gas has to be cleaned until it does not contain more sulphur than exhaust gas from a low-sulphur fuel. The sulphur limit was recently cut to a maximum of 0.1 % S in the fuel burned in SECAs. As a consequence, ships use low sulphur fuels or installed scrubbers on board that clean the exhaust gas from sulphur and other contaminants. Outside SECAs, the allowed sulphur content in ship fuels is currently at 3.5 %, but it will be reduced to 0.5 % in 2020 or 2025 at the latest. The exact date will be decided in 2018 when the availability of ship fuel containing less than 0.5 % S will be reviewed.

Nitrogen oxide emissions from ships are also regulated in MARPOL Annex VI. Since the year 2000 the $NO_x$ limits for ships built after 1 January 2000 are 17 g $kWh^{-1}$ $NO_x$ (Tier I regulation). In 2010 the second step (Tier II) of the $NO_x$ regulations came into force with an emission factor of 14.4 g $kWh^{-1}$ $NO_x$ for new ships. The third step (Tier III), when $NO_x$ limits will be further reduced to 3.5 g $kWh^{-1}$ $NO_x$, is planned for 2016 for the ECAs around North America. However, this will only be applied to new ships sailing in designated Emission Control Areas while Tier I and Tier II represent global limits. The North Sea and the Baltic Sea are in discussion to become such an ECA for $NO_x$. However, Tier III rules will only be valid for ships built after the designation date (International Maritime Organisation, Marine Environment Protection Committee, 2014). Until now, it is unclear when this date will be.

In the European project Clean North Sea Shipping (CNSS) different technologies capable of reducing air emissions from ships in the North Sea were investigated. Among them are scrubbers that reduce sulphur emissions, catalysts that reduce $NO_x$ emissions and the use of alternative fuels like liquefied natural gas (LNG). In order to es-





ACPD
15, 11325–11368, 2015

timate the effect of these technologies and of legislation on $NO_x$ and $SO_2$ emissions from ships, emission scenarios were developed for the year 2030. These scenarios consider the same development of the world fleet and different developments in legislation and the use of alternative fuels. The basis is a detailed emission inventory for the year 2011 which is built upon AIS (Automatic Identification System) ship positions and a detailed ship characteristics data base (Aulinger et al., 2015). The scenarios are implemented as modified emission inventories for the year 2030. The inventories serve as input for the chemistry transport model CMAQ that is setup for the North Sea region. CMAQ calculates transport and transformation of the emitted pollutants and finally yields concentration maps that illustrate the impact of shipping emissions on the air quality in the North Sea region.

## 2 Ship emission inventories

### 2.1 Reference emissions

The basis for the ship fleet and the ship movements on the North Sea is a data set with AIS positions of ships for the entire year 2011 combined with a ship characteristics data base that includes all ships given in the AIS data set. The data is used to calculate the energy demand of individual ships depending on the installed engine and their actual velocity. From this, fuel use as well as $NO_x$, $SO_2$, $CO_2$, CO, Hydrocarbon (HC), and Particulate Matter (PM) emissions are calculated with load-dependent emission factors for the different species. For the first time, load dependent emission factors resulting from test bed measurements of about 250 different ship engines were used to calculate a ship emission inventory. For the details, the reader is directed to the accompanying paper by Aulinger et al. (2015).





ACPD
15, 11325–11368, 2015

## 2.2 Scenario description

The purpose of scenarios is to describe plausible and possible future developments. Scenarios are often used to describe the boundaries of possible future situations, e.g. a worst case and a best case. In our study we decided to create scenarios that describe the future development of policy and technology regarding exhaust gas emissions from ships in the North Sea area. We adopted the methodology described in (Eyring et al., 2005) for our scenarios and distinguish between traffic demand and future technological and legislative developments. However, because we focus on the implementation of a $NO_x$ emission control area in the North Sea, we take only one scenario for the fleet development into account as a basis as it is described in publications from IMO (Buhaug et al., 2009; Smith et al., 2014) and Det Norske Veritas (Det Norske Veritas, 2012). Taking multiple possible developments of the world trade into account would add too much complexity to the scenarios.

In brief, our fleet development scenario assumes an increase in the number of bigger ships while the number of smaller ships decreases in the North Sea area. This leads to an increase in ship number by 1.0 % $year^{-1}$ and an increase in transported cargo of 2.5 % $year^{-1}$ Additional to this increase in ship number it is assumed that per year 2.5 % of all ships are replaced by new ones, no matter of what size they are. The main techniques under investigation are Liquefied Natural Gas (LNG) as an alternative fuel for shipping and end-of-the-pipe technologies like scrubbers and Selective Catalytic Reduction (SCR) to reduce sulphur dioxide and nitrogen oxide emissions.

The main drivers for changes in the use of ship fuels and in the amount of emissions to air are on the one hand regulations, and here mainly what is written in MARPOL Annex VI (International Maritime Organisation, 2008), and on the other hand the price of different fuels. Therefore, the main scenarios include strict and less strict legislations as one axis and the price of LNG compared to Marine Gas Oil (MGO) or Heavy Fuel Oil (HFO) as the second axis. Some regulations in MARPOL Annex VI (those related to $NO_x$ emissions) are only valid for newly built ships after a certain date, depending on





ACPD
15, 11325–11368, 2015

the region where the ECA is located. The earliest date when Tier III $NO_x$ regulations will come into force is 1 January 2016. For the North Sea and the Baltic Sea, it is likely that Tier III $NO_x$ regulations will be implemented significantly later than 2016.

Because the $NO_x$ regulations apply only to new ships means that it needs some time until a considerably higher number of ships in the fleet will have reduced $NO_x$ emissions. Those regulations related to the sulphur content in ship fuels apply to all ships, and should have immediate effects on the total emissions of sulphur oxides. To particularly take into account the long term effects of new ships following Tier III regulations, the year 2030 is used in the scenarios as target year. The development of the world fleet until 2030 compared to the reference year 2011 is considered.

These drivers are combined into six scenarios that can be arranged in a coordinate system with legislation on the $x$ axis and LNG price on the $y$ axis (see Fig. 1). Different implementation dates for $NO_x$ Tier III rules (2016 and 2021) are chosen.

The stories behind these scenarios can be described as follows:

### 2.2.1 Scenario No ECA

The global economy suffers from low GDP growth rates and in order to avoid additional costs for the shipping industry some regulations will not be implemented (global $SO_x$ limit, $NO_x$ limits in ECAs). This can be considered as the worst case scenario, however 0.1 % S in fuels in ECAs will still be implemented.

### 2.2.2 Scenarios ECA SCR 16 and ECA SCR 21

All regulations currently given in MARPOL Annex VI will be in force. The global sulphur limit of 0.5 % S in fuel will be in force by 2020, in ECAs a sulphur limit of 0.1 % S will be implemented since 2015. A $NO_x$ emission control area will be implemented in the North and Baltic Seas. Two different years, 2016 and 2021, are considered as implementation dates. LNG is expensive and the LNG infrastructure is not built up to provide LNG to many ships. Therefore ship owners will prefer low sulphur fuels and catalysts (SCR)





ACPD
15, 11325–11368, 2015



V. Matthias et al.

or exhaust gas recirculation systems (EGR) to comply with the rules. Some will use scrubbers only, if they do not have to follow the Tier III regulations (older ships).

### 2.2.3 Scenarios ECA LNG 16 and ECA LNG 21

The legislation is the same as in scenarios ECA SCR 16 and ECA SCR 21 but LNG will be the cheaper solution to comply with the rules. In 2030, about 6000 ships in the North Sea will run on LNG. Ships that sail more than 50 % of the time in the North and Baltic Seas will preferably use LNG. Some newer ships will also be retrofitted with LNG engines.

### 2.2.4 Scenario ECA opt

This is built on scenario ECA SCR but it assumes that the strict rules for $NO_x$ emissions for new-buildings will also apply to older ships in 2030. They will then be retrofitted with exhaust gas cleaning systems in order to follow these rules. This is regarded as the best case scenario and illustrates the reduction potential. However, exhaust gas cleaning systems increase the fuel consumption, so the fuel use in this scenario will be higher than in the previous scenarios in which only parts of the ships are equipped with exhaust gas cleaning.

## 2.3 Future shipping emissions

The emission inventories that were constructed as input for the CMAQ model were developed from the ship emission inventory for 2011 which is based on AIS data and ship characteristics data. First, the fleet development was applied. Then, the new emissions were calculated by using modified emission factors for the specific emissions of the ships. All emission factors are given in $g\,kWh^{-1}$ for the different substances under investigation, they have been reduced depending on the scenario and taking into account the age of the different ships in the scenarios ECA SCR and ECA LNG. In particular, in all scenarios it has been taken into account that a fraction of the older





ACPD
15, 11325–11368, 2015
Impact of shipping emissions: scenarios for 2030
V. Matthias et al.

ships, that do not have to follow any of the Tier rules for $NO_x$ emissions, are taken out of service until 2030 and will be replaced by ships following Tier II. In areas where no AIS data was available (e.g. west of France), shipping emissions as given in the EMEP inventory were used.

The change of the annual average emissions for $NO_x$ and $SO_x$ in comparison to the reference emissions of 2011 are given for the scenarios in Figs. 2 and 3, respectively. Regional differences in the emission changes are a result of ship types and ship sizes which undergo different temporal developments in fleet renewal. This depends on the actual age of the ships given in the ship characteristics data base.

## 3 Chemistry transport modeling

### 3.1 CMAQ

The CMAQ model (Byun and Ching, 1999; Byun and Schere, 2006) was used in its version 4.7.1 with the CB05 chemistry mechanism. Compared to its previous version, the model update includes several new features (Foley et al., 2010), among them are gas phase chlorine chemistry, improved secondary organic aerosol (SOA) formation (Edney et al., 2007) and an updated representation of sea salt that considers reactions with nitric acid and the formation of coarse mode nitrate (Kelly et al., 2010) in the so-called AE5 aerosol mechanism. The model was run for an entire year with a spinup time of 2 weeks. Standard profiles for the most important atmospheric pollutants were used as initial conditions. However, their effect on the simulated atmospheric concentrations of the substances in focus in this paper is negligible after the spinup.

The model was setup on a 72 km × 72 km grid for entire Europe and subsequently on a nested 24 km × 24 km grid for central Europe, see Fig. 4. The vertical model extent contains 30 layers up to 100 hPa in a sigma hybrid pressure coordinate system. 20 of these layers are below approx. 2 km, the lowest layer extends to ca. 36 m above ground. The evaluation area was restricted to the Greater North Sea region and some neigh-



ACPD
15, 11325–11368, 2015

bouring section of the NE Atlantic, covering approximately half of the central European domain (see the red box in Fig. 4).

### 3.2 COSMO-CLM

The meteorological fields that drive the chemistry transport model were simulated with the COSMO-CLM mesoscale meteorological model (version 4.8) for the year 2008 (Geyer, 2014) using NCEP forcing data (Kalnay et al., 1996). This year was chosen because it does not contain very unusual meteorological conditions in Europe and can therefore be used to represent typical weather conditions in Europe. The same meteorological fields were used for the scenario runs, i.e. projected changes due to climate change were not considered in order to avoid a mixture of effects, from emissions and meteorological data, in the resulting concentrations of air pollutants.

COSMO-CLM is the climate version of the regional scale meteorological community model COSMO (Rockel et al., 2008), originally developed by Deutscher Wetterdienst (DWD) (Steppeler et al., 2003; Schaettler et al., 2008). It has been run on a $0.22^{\circ} \times 0.22^{\circ}$ grid using 40 vertical layers up to 20 hPa for entire Europe. COSMO-CLM uses the TERRA-ML land surface model (Schrodin and Heise, 2001), a TKE closure scheme for the planetary boundary layer (Doms, 2011; Doms et al., 2011), cloud microphysics after Seifert and Beheng (2001, 2006), the Tiedtke scheme (Tiedtke, 1989) for cumulus clouds and a long wave radiation scheme following Ritter and Geleyn (1992). The meteorological fields were afterwards processed to match the CMAQ grid. As far as possible, CMAQ uses the information that is provided by the meteorological input fields to calculate transport, transformation and loss of all gas phase and particulate species. The impact of the meteorological fields on the output of the chemistry transport model was investigated in detail in the articles by Matthias et al. (2009) and Bieser et al. (2011a).





ACPD
15, 11325–11368, 2015

## 3.3 Boundary conditions

Chemical boundary conditions for the outer model domain were taken from monthly means of the TM5 global chemistry transport model system (Huijnen et al., 2010) and were provided by the Dutch Royal Meteorological Institute (KNMI). The model results have been interpolated in time and space to provide daily boundary conditions for the 72 km × 72 km CMAQ grid for Europe. Boundary conditions for the nested 24 km × 24 km grid were calculated on hourly basis from the outer coarse grid. They were kept the same for all scenarios in order to restrict the analysis of the effects of emission changes on shipping in North Western Europe.

## 3.4 Land based emissions

The model runs were performed with full emissions from all relevant sources in the model domain. Land based emissions in hourly temporal resolution were produced with SMOKE EU (Bieser et al., 2011a) for the year 2011. They are based on officially reported EMEP emissions which are distributed in time and space using appropriate surrogates like population density, street maps or land use. Point sources were considered as far as information from the European point source emission register was available. The vertical distribution of the emissions was calculated online with the SMOKE model, the results are given by Bieser et al. (2011b). The land based emissions were kept constant for all scenario model runs. Therefore the impact of reduced land based emissions, which can be expected for Europe in the year 2030, was not considered here. This was done to keep the the analysis clear and discuss only the effects of shipping instead of mixing it up with reductions of land based sources.





ACPD
15, 11325–11368, 2015

## 4 Impact of shipping on concentrations of pollutants

### 4.1 Situation today

The results for today's air pollution due to shipping serve as a reference case for this study. They are discussed in detail in the accompanying paper by Aulinger et al. (2015). In brief it can be said that ships contribute significant amounts to the concentrations of $NO_2$, particle bound nitrate ($NO_3^-$ (p)) and particle bound sulphate ($SO_4^{2-}$ (p)). In summer, ozone is enhanced, too. High contributions from shipping to the $NO_2$ and $SO_2$ concentrations are restricted to the open sea and the coastal areas in the southern North Sea and in Denmark (see the reference case in Figs. 5 and A1). Nitrate and sulphate aerosol particles as well as ozone are secondary pollutants. They are transported far more inland but their relative contribution to concentrations at the coast is lower compared to $NO_2$ and $SO_2$.

There are large differences between summer and winter. As a photochemical pollutant, ozone is only increased during the summer months. The situation is similar for sulphate and nitrate aerosol. Both are formed via oxidation path ways that include the photochemically formed OH radical. Therefore, the conversion rate of $SO_2$ into $SO_4^{2-}$ (p) and of $NO_2$ into $NO_3^-$ (p) in summer is higher than in winter. This leads to higher contributions of shipping emissions to the concentrations of these aerosol components in summer. On the other hand, total nitrate aerosol concentrations are much lower in summer compared to winter, because the gas-to-particle partitioning between $HNO_3$ and $NO_3^-$ (p) is temperature dependent with higher particulate nitrate concentrations at low temperatures.

### 4.2 Scenarios for the North Sea in 2030

We mainly discuss the consequences of changes in the $NO_x$ emissions from ships because here we see the main differences between the scenarios (Fig. 2). Additionally, the strict rules for $SO_2$ came into force in the North Sea ECA on 1 January 2015, and





ACPD
15, 11325–11368, 2015

there are only small differences between the scenarios with respect to $SO_2$ emissions in the North Sea (Fig. 3). This will be further discussed in Sect. 4.2.4.

$NO_x$ emissions from ships have an impact on the $NO_2$ concentrations, on nitrate aerosol and on ozone. It can be expected that $NO_2$ concentrations increase due to ship emissions. The impact of $NO_x$ emissions from ships on ozone will be different between winter and summer. While in summer increased $NO_x$ emissions will lead to increased ozone under most weather conditions and in most regions, this will have almost no effect in winter.

In the following, maps illustrating changes in the contribution of shipping on $NO_2$, nitrate aerosol and ozone concentrations in 2030 will be shown for the scenarios No ECA, ECA SCR 16 (Tier III in 2016), ECA SCR 21 (Tier III in 2021) and ECA opt. The color coded relative changes refer to the impact of the shipping emissions on the concentrations of selected pollutants. The latter is given in reference maps which are results of the reference model run considering shipping emissions from 2011. The changes in the other scenarios will be illustrated in time series for different North Sea coastal regions (see Fig. 4), each of them comprising about 9200 $km^2$. These time series nicely show the highly variable impact of shipping emissions, which depends to a large extent on the weather conditions and the concentrations of pollutants from other sources.

### 4.2.1 Nitrogen dioxide

Scenario No ECA is reflecting a steady increase in shipping activity disregarding the implementation of stricter rules for $NO_x$ emissions. This will lead to an increase in the contribution of shipping to the average $NO_2$ concentrations by more than 30 % in large areas of the North Sea region (Fig. 5b). The largest increase can be seen in the English Channel and the south western North Sea while Norway and Sweden exhibit lower increase rates of around 20 %.

Figure 5c displays scenario ECA SCR 21 in which the Tier III rules for new ships come into force in 2021. This means that in 2030 a large part of the fleet will still follow





ACPD
15, 11325–11368, 2015

the less strict Tier I and Tier II regulations. Very few ships older than 30 years will not have to comply with any of the $NO_x$ regulations. As a consequence, the contribution of ships to average $NO_2$ concentratios will be higher than in the case with Tier III regulations from 2016 onwards (Fig. 5d). In large parts of the North Sea the contribution of shipping to $NO_2$ concentrations will be higher than today.

Scenario ECA SCR 16 on average still shows a moderate increase in the $NO_2$ concentrations caused by ships compared to the situation today (Fig. 5d). While in the English Channel and the southern North Sea the concentrations decrease by a few percent only, they decrease by more than 10 % in the north western parts of the North Sea and in particular at the British, Norwegian and Swedish coast. This is caused by the fact that the traffic to the main North Sea ports in Rotterdam, Hamburg and Antwerp will still increase and ships will become bigger, resulting in a rather small concentration decrease in the English Channel. Today, smaller and older ships travel to the smaller harbours in the North Sea area. However, many of them will be replaced after 2016, which means that a large fraction of those ships will comply with Tier III. This will lead to a reduction of the contribution of shipping emissions to $NO_2$ concentrations in the central and northern part of the North Sea.

The contribution of shipping to $NO_2$ concentrations will be drastically reduced in the case of scenario ECA opt when all ships comply with Tier III rules for $NO_x$ emissions (Fig. 5e). The simulations show a reduction of approximately 80 % all over the North Sea region compared to today.

All reductions in the contribution of shipping to $NO_2$ concentrations have a similar magnitude and regional distribution in winter and summer. On average the impact of shipping is slightly higher in winter compared to summer with a larger increase in scenario No ECA and ECA SCR 21 and a smaller decrease in scenario ECA SCR 16 and ECA opt. All maps for the winter case can be seen in the Appendix (Fig. A3).

Figure 6 shows a time series of the contribution of shipping to the daily average $NO_2$ concentrations at the coasts of Belgium and the Netherlands (see Fig. 4 for the region). Of the scenarios for 2030, scenario ECA SCR 16 shows a slight decrease in





ACPD
15, 11325–11368, 2015

the contribution of shipping to the $NO_2$ concentrations compared to today. If Tier III will be implemented in 2021 (scenario ECA SCR 21) or not at all until 2030 (scenario No ECA), the contribution of shipping to the $NO_2$ concentration will be higher than today. Large reductions of $NO_2$ from shipping, on some days more than 4 µg m$^{-3}$, are only achieved when all ships and not only new-buildings follow the Tier III regulations. Time series for the other region are included in the Appendix (Fig. A6).

#### 4.2.2 Nitrate aerosol

Nitrate aerosol ($NO_3^-$ (p)) is formed in the atmosphere as a consequence of the oxidation of $NO_2$. The amount of aerosol particles formed highly depends on the presence of other pollutants, in particular on the availability of ammonia ($NH_3$). Ammonia mainly stems from agricultural activities. The regions with the highest ammonia emissions are western France, the Benelux countries, western Germany and Denmark. Particulate ammonium nitrate preferentially exists in winter, at low temperatures. At higher temperatures ammonium nitrate particles decompose into gaseous ammonia and nitric acid. Therefore, nitrate aerosol concentrations all over Europe are much lower in summer compared to winter. On the other hand, oxidation of $NO_2$ is much more effective in summer leading to a higher contribution of shipping to nitrate aerosol compared to winter.

In summer, the emission scenarios show very similar results for nitrate aerosol and for $NO_2$ (see Fig. 7). In scenario No ECA the contribution of shipping to nitrate aerosol concentrations increases by more than 30 % over sea and by 25 % or more in large aeras of central Europe and in southern Scandinavia (Fig. 7b). In scenario ECA SCR 21 (Fig. 7c) large areas of the North Sea, and in particular northern France, show an increase in nitrate aerosol from shipping while in other areas the situation will remain unchanged. Scenario ECA SCR 16 (Fig. 7d) shows a decrease in the contribution of shipping to nitrate aerosol concentrations by 7–10 % in the north eastern part of the North Sea while in the south western part a small increase by 5–10 % can be observed.





ACPD
15, 11325–11368, 2015

Again, in scenario ECA opt the contribution of shipping to nitrate aerosol will be reduced by 60–80 %.

In winter, nitrate aerosol concentrations are only marginally affected by shipping emissions. For this reason the results of the scenario runs do not show reliable patterns of changes in $NO_3^-$ (p) concentrations caused by changing shipping emissions when given as relative changes. Therefore, they are not shown.

### 4.2.3 Ozone

$NO_x$ emissions from ships have a strong influence on the atmospheric ozone concentrations. Ozone is formed out of $NO_2$ and atmospheric oxygen in the presence of sunlight. Volatile organic compounds (VOC) help to transform emitted NO into $NO_2$, thereby enhancing the ozone formation significantly. On the other hand NO destroys ozone, leading to low ozone concentrations during night-time when no photolysis of $NO_2$ takes place. This leads to a strong diurnal cycle of the ozone concentration and a large difference between winter and summer levels with much higher ozone concentrations in the summer. Furthermore, increased $NO_x$ emissions may cause additional ozone formation in presence of sufficiently high VOC concentrations. If the VOC levels are comparably low, more $NO_x$ causes ozone destruction.

Here, we look at the impact of shipping emissions on the daily mean ozone values. Figure 8 shows maps of the distribution of changes in the contribution of ships to mean ozone concentration for the different scenarios. Figure 8a shows that shipping causes about 7 $\mu g\,m^{-3}$ additional ozone (summer average value) in large parts of the North Sea and in Denmark. On the other hand, there is only a small increase in ozone in the English Channel, where $NO_x$ concentrations are high. The effect of ozone destruction by additional $NO_x$ emissions under low VOC conditions can be clearly seen in scenario No ECA (Fig. 8b). Reductions in ozone concentrations caused by shipping emissions, by partly more than 80 %, are clearly noticeable in the English channel, the south western North Sea and the surrounding coast line. On the other hand, the ship-





ACPD
15, 11325–11368, 2015

ping contribution to increased ozone concentrations will be enhanced by more than 20 % far from the main shipping areas in Central Europe, Ireland and the Northern UK.

Scenario ECA SCR 21 (Fig. 8c) contains higher $NO_x$ emissions, leading to decreased ozone in the English channel and higher values in Central Europe, France, Ireland and the UK. Scenario ECA SCR 16 (Fig. 8d) shows a lower shipping contribution to ozone concentrations in the North East of the North Sea region and an almost unchanged situation in the South West. In the case of ECA opt, ozone caused by shipping emissions is significantly reduced by 40–60 % all over the modeling domain, except for the English channel where a significant increase is found.

Figure 9 displays a time series of the daily average ozone concentrations in northern Germany. It can be seen that the ozone values would be lower in summer, on some days more than 10 $\mu g\,m^{-3}$, if ships emitted as little $NO_x$ as in the ECA opt scenario. On the other hand they would be slightly higher in winter.

An analysis of the different regions reveals that the days with concentrations higher than 120 $\mu g\,m^{-3}$ (a value recommended by the World Health Organization, WHO) would decrease significantly by 50 % or more without shipping emissions in all regions except the Netherlands (see Table 1). The scenarios for 2030 do not show big differences in the number of days with concentrations above 120 $\mu g\,m^{-3}$. While small increases in the number of days can be expected if Tier III rules were not implemented (scenario No ECA), the only case with a strong decrease in exceedance days is scenario ECA opt.

#### 4.2.4 Sulphur dioxide and sulphate aerosol

Sulphur dioxide ($SO_2$) emissions from ships are directly related to the sulphur content of ship fuels. In the scenarios for 2030 all ships will follow the same rules for sulphur, which allow 0.1 % S in the fuel in the North and Baltic Sea ECA and 0.5 % outside of it. Therefore, the scenarios do not differ much in terms of sulphur emissions. The main difference is between the ECA SCR and ECA LNG scenarios, because LNG does not contain any sulphur at all which makes the sulphur emissions from these ships even lower than for all other ships that comply with the 0.1 % S rule inside the North Sea area.

In Fig. 10 changes in the contribution from shipping to the $SO_2$ and $SO_4$ concentrations for the scenario ECA SCR 16 and ECA LNG 16 are shown for summer. In the ECA LNG 16 scenario sulphur dioxide and sulphate aerosol concentrations are even further reduced than in the ECA SCR 16 scenario. The reductions are between 40 and 60 % for the SCR case and between 60 and 80 % for the LNG case. The reductions are slightly higher for $SO_2$ compared to sulphate, however the reductions for sulphate are more widespread than those for $SO_2$. The results for the other scenarios are very close to those in Fig. 10 which is why they are not shown here. More maps are included in the Appendix (Figs. A1, A2, A4 and A5).

#### 4.2.5 $PM_{2.5}$

Particulate matter with a diameter less than 2.5 µm ($PM_{2.5}$) originating from shipping emissions is mainly formed through a conversion of gaseous $SO_2$ and $NO_2$ into particulate nitrate ($NO_3^-$ (p)) and sulphate ($SO_4^{2-}$ (p)). The amount of these secondary aerosol components depends critically on the level of $NH_3$ emissions, which are a prerequisite for the formation of ammonium sulphate and annomium nitrate in the atmosphere. The area where the highest contribution of shipping to the $PM_{2.5}$ concentrations is noticeable is south east of the main shipping lanes, in North West France, Belgium, the Netherlands and North Germany. These are areas with high ammonia emissions from agricultural activities.

Reductions in the contribution of shipping to $PM_{2.5}$ are visible in all scenarios (see Fig. 11). This is caused by the significant effect the sulphur reductions in the ship fuel has on sulphate aerosol concentrations. In scenario ECA opt the $PM_{2.5}$ reduction is the largest. Here, also nitrate aerosol is significantly reduced.

The time series for $PM_{2.5}$ concentrations and the respective reductions in the different scenarios can be seen for Northern Germany in Fig. 12. All scenarios except for No ECA show reductions in $PM_{2.5}$ on almost all days. Again, the largest reductions can





ACPD
15, 11325–11368, 2015

be seen for ECA opt. There is no clear seasonal trend for the reductions although total $PM_{2.5}$ is higher in winter compared to summer.

## 5 Conclusions

This paper investigates the effects of different future developments of shipping emissions in the North Sea area on air quality in the North Sea region. The main differences between the scenarios for 2030 concern nitrogen oxide emissions. They could be significantly lowered by using exhaust cleaning techniques or alternative fuels like LNG. Additionally, international regulations for a mandatory reduction of nitrogen oxide emissions in the North and Baltic Sea areas are under debate in the International Maritime Organization.

It was found that the expected increase in ship traffic in the North Sea will lead to enhanced levels of $NO_2$, nitrate aerosol and ozone in large areas of North West France, Belgium, the Netherlands, North Germany and Denmark if no emission reduction measures will be taken. For secondary pollutants like ozone and aerosols, this effect is more pronounced in summer compared to winter. In winter shipping does not contribute much to elevated levels of aerosol concentrations.

The effect of emission reduction measures depends on the year of implementation. If already in 2016 new ships needed to follow the new Tier III rules for new-buildings, the concentrations of $NO_2$, nitrate aerosol and ozone in 2030 would be on the same level as today. This means that the emission reductions of the new ships are compensated by an increased ship traffic. If it took another five years until Tier III regulations were in place, the concentrations of $NO_2$, nitrate aerosol and ozone which are caused by ship traffic would be higher in 2030 compared to today. The difference to the implementation of the Tier III rules in 2016 would be about 10–15 %. Significant reductions can only be achieved if all ships, not only new-buildings, followed strict $NO_x$ emission limitations.

The situation is different for sulphur dioxide, sulphate aerosol particles and also for $PM_{2.5}$. Regulations on lower sulphur levels in ship fuels have been implemented on 1





ACPD
15, 11325–11368, 2015

January 2015 for the North Sea and will be in place for all seas in 2020 (or the latest in 2025). This will significantly reduce the impact of shipping on $SO_2$ and sulphate aerosol concentrations. As a consequence of lower sulphate aerosol concentrations $PM_{2.5}$ concentrations will also be reduced. The use of LNG as alternative fuel would further reduce sulphur emissions and therefore also $SO_2$ and $PM_{2.5}$ concentrations.

Our model study shows that all effects of shipping emissions on air quality differ largely by region and season, depending on the pollutant in focus. Gaseous primary pollutants like $NO_2$ and $SO_2$ have a short life time. Consequently, their effects can mainly be seen close to the shipping lanes. Aerosols, which are formed through oxidation in the atmosphere can be transported over large distances. Contributions of shipping to nitrate, sulphate and $PM_{2.5}$ concentrations can be seen far inland. For ozone, future emission reductions of $NO_x$ could even lead to enhanced concentrations in regions that already today have high $NO_x$ and low VOC concentrations like in the English Channel. However, this will depend on the future development of other $NO_x$ emission sources, too. These were not taken into account here, as has been done for climate change neither, in order to focus on shipping effects and facilitate the interpretation of emission changes in this sector. Because it can be expected that all land based anthropogenic emissions in Europe will decrease considerably until 2030, the relative contribution of shipping emissions to pollution levels in the North Sea area might be even higher than demonstrated here.

*Acknowledgements.* This work has partly been funded by the European Regional Development Fund (ERDF) within the Interreg IVB projects Clean North Sea Shipping (CNSS) and CNSS Improved Dissemination and Impact (CNSS-IDI). We thank our colleagues from CNSS for their valuable comments concerning the development of the emission scenarios.

US EPA is gratefully acknowledged for the use of CMAQ, we thank Twan van Noije (KNMI) for providing TM5 model data.

The article processing charges for this open-access publication were covered by a Research Centre of the Helmholtz Association.





ACPD

15, 11325–11368, 2015

## References

Aulinger, A., Matthias, V., Zeretzke, M., Bieser, J., Quante, M., and Backes, A.: The impact of shipping emissions on air pollution in the Greater North Sea region – Part 1: Current emissions and concentrations, Atmos. Chem. Phys. Discuss., 15, 11277–11323, doi:10.5194/acpd-15-11277-2015, 2015. 11326, 11328, 11335

Bieser, J., Aulinger, A., Matthias, V., Quante, M., and Builtjes, P.: SMOKE for Europe – adaptation, modification and evaluation of a comprehensive emission model for Europe, Geosci. Model Dev., 4, 47–68, doi:10.5194/gmd-4-47-2011, 2011a. 11333, 11334

Bieser, J., Aulinger, A., Matthias, V., Quante, M., and Denier van der Gon, H. A. C.: Vertical emission profiles for Europe based on plume rise calculations, Environ. Pollut., 159, 2935–2946, doi:10.1016/j.envpol.2011.04.030, 2011b. 11334

Buhaug, Ø., Corbett, J., Endresen, Ø., Eyring, V., Faber, J., Hanayama, S., Lee, D., Lee, D., Lindstad, H., Markowska, A., Mjelde, A., Nelissen, D., Nilsen, J., Pålsson, C., Winebrake, J., Wu, W., and Yoshida, K.: Second IMO GHG Study, Tech. rep., International Maritime Organization (IMO), London, UK, 2009. 11329

Byun, D. and Ching, J.: Science Algorithms of the EPA Models-3 Community Multiscale Air Quality Modeling System, Epa/600/r-99/030, US Environmental Protection Agency, Office of Research and Development, Washington DC, 1999. 11332

Byun, D. and Schere, K.: Review of the governing equations, computational algorithms, and other components of the Models-3 Community Multiscale Air Quality (CMAQ) modeling system, Appl. Mech. Rev., 59, 51–77, 2006. 11332

Det Norske Veritas: DNV Report Shipping 2020, Tech. rep., DNV, Høvik, Norway, 2012. 11329

Doms, G.: A Description of the Nonhydrostatic Regional COSMO model. Part I: Dynamics and Numerics., Tech. rep., Deutscher Wetterdienst, available at: http://www.cosmo-model.org/content/model/documentation/core/cosmoDyncsNumcs.pdf (last access: 8 April 2015), 2011. 11333

Doms, G., Förstner, J., Heise, E., Herzog, H.-J., Mrionow, D., Raschendorfer, M., Reinhart, T., Ritter, B., Schrodin, R., Schulz, J.-P., and Vogel, G.: A Description of the Nonhydrostatic Regional COSMO Model. Part II: Physical Parameterization, Tech. rep., Deutscher Wetterdienst, available at: http://www.cosmo-model.org/content/model/documentation/core/cosmoPhysParamtr.pdf (last access: 8 April 2015), 2011. 11333





ACPD
15, 11325–11368, 2015

Impact of shipping emissions: scenarios for 2030

V. Matthias et al.

Edney, E. O., Kleindienst, T. E., Lewandowski, M., and Offenberg, J. H.: Updated SOA chemical mechanism for the Community Multi-Scale Air Quality model, Tech. Rep. EPA 600/X-07/025, US EPA, Research Triangle Park, NC, 2007. 11332

Eyring, V., Kohler, H. W., Lauer, A., and Lemper, B.: Emissions from international shipping: 2. Impact of future technologies on scenarios until 2050, J. Geophys. Res.-Atmos., 110, D17306, doi:10.1029/2004JD005620, 2005. 11329

Foley, K. M., Roselle, S. J., Appel, K. W., Bhave, P. V., Pleim, J. E., Otte, T. L., Mathur, R., Sarwar, G., Young, J. O., Gilliam, R. C., Nolte, C. G., Kelly, J. T., Gilliland, A. B., and Bash, J. O.: Incremental testing of the Community Multiscale Air Quality (CMAQ) modeling system version 4.7, Geosci. Model Dev., 3, 205–226, doi:10.5194/gmd-3-205-2010, 2010. 11332

Geyer, B.: High-resolution atmospheric reconstruction for Europe 1948–2012: coastDat2, Earth Syst. Sci. Data, 6, 147–164, doi:10.5194/essd-6-147-2014, 2014. 11333

Hammingh, P., Holland, M., Geilenkirchen, G., Jonson, J., and Maas, R.: Assessment of the environmental impacts and health benefits of a nitrogen emission control area in the North Sea, Tech. rep., PBL Netherlands Environmental Assessment Agency, The Hague, 2012. 11326

Huijnen, V., Williams, J., van Weele, M., van Noije, T., Krol, M., Dentener, F., Segers, A., Houweling, S., Peters, W., de Laat, J., Boersma, F., Bergamaschi, P., van Velthoven, P., Le Sager, P., Eskes, H., Alkemade, F., Scheele, R., Nédélec, P., and Pätz, H.-W.: The global chemistry transport model TM5: description and evaluation of the tropospheric chemistry version 3.0, Geosci. Model Dev., 3, 445–473, doi:10.5194/gmd-3-445-2010, 2010. 11334

International Maritime Organisation: Amendments to the Annex of the Protocol of 1997 to Amend the International Convention for the Prevention of Pollution from Ships, 1973, as Modified by the Protocol of 1978 Relating thereto (MARPOL Annex VI), available at: http://www.imo.org/blast/blastDataHelper.asp?data_id=23760&filename=176 (last access: 8 April 2015), 2008. 11327, 11329

International Maritime Organisation, Marine Environment Protection Committee: http://www.imo.org/MediaCentre/MeetingSummaries/MEPC/Pages/MEPC66.aspx (last access: 25 January 2015), 2014. 11327

Jalkanen, J.-P., Johansson, L., Kukkonen, J., Brink, A., Kalli, J., and Stipa, T.: Extension of an assessment model of ship traffic exhaust emissions for particulate matter and carbon monoxide, Atmos. Chem. Phys., 12, 2641–2659, doi:10.5194/acp-12-2641-2012, 2012. 11326





ACPD
15, 11325–11368, 2015

Kalnay, E., Kanamitsu, M., Kistler, R., Collins, W., Deaven, D., Gandin, L., Iredell, M., Saha, S., White, G., Woollen, J., Zhu, Y., Chelliah, M., Ebisuzaki, W., Higgins, W., Janowiak, J., Mo, K. C., Ropelewski, C., Wang, J., Leetmaa, A., Reynolds, R., Jenne, R., and Joseph, D.: The NCEP/NCAR 40-year reanalysis project, B. Am. Meteorol. Soc., 77, 437–471, 1996. 11333

Kelly, J. T., Bhave, P. V., Nolte, C. G., Shankar, U., and Foley, K. M.: Simulating emission and chemical evolution of coarse sea-salt particles in the Community Multiscale Air Quality (CMAQ) model, Geosci. Model Dev., 3, 257–273, doi:10.5194/gmd-3-257-2010, 2010. 11332

Matthias, V., Quante, M., and Aulinger, A.: Determination of the optimum MM5 configuration for long term CMAQ simulations of aerosol bound pollutants in Europe, Environ. Fluid Mech., 9, 91–108, doi:10.1007/s10652-008-9103-6, 2009. 11333

Matthias, V., Bewersdorff, I., Aulinger, A., and Quante, M.: The contribution of ship emissions to air pollution in the North Sea regions, Environ. Pollut., 158, 2241–2250, doi:10.1016/j.envpol.2010.02.013, 2010. 11326

Ritter, B. and Geleyn, J. F.: A comprehensive radiation scheme for numerical weather prediction models with potential applications in climate simulations, Mon. Weather Rev., 120, 303–325, doi:10.1175/1520-0493(1992)120<0303:ACRSFN>2.0.CO;2, 1992. 11333

Rockel, B., Will, A., and Hense, A.: The regional climate model COSMO-CLM(CCLM), Meteorol. Z., 17, 347–348, 2008. 11333

Schaettler, U., Doms, G., and Schraff, C.: A Description of the Nonhydrostatic Regional COSMO-Model Part VII: User's Guide, Tech. rep., Deutscher Wetterdienst, 2008. 11333

Schrodin, R. and Heise, E.: The multi-layer-version of the DWD soil model TERRA/LM, Tech. Rep, Consortium for Small-Scale Modelling (COSMO), available at: http://www.cosmo-model.org/content/model/documentation/techReports/docs/techReport02.pdf (last access: 8 April 2015), 2001. 11333

Seifert, A. and Beheng, K. D.: A double-moment parameterization for simulating autoconversion, accretion and selfcollection, Atmos. Res., 59–60, 265–281, doi:10.1016/S0169-8095(01)00126-0, 2001. 11333

Seifert, A. and Beheng, K. D.: A two-moment cloud microphysics parameterization for mixed-phase clouds. Part 1: Model description, Meteorol. Atmos. Phys., 92, 45–66, 2006. 11333

Smith, T. W. P., Jalkanen, J. P., Anderson, B. A., Corbett, J. J., Faber, J., Hanayama, S., O'Keeffe, E., Parker, S., Johansson, L., Aldous, L., Raucci, C., Traut, M., Ettinger, S., Nelis-





ACPD
15, 11325–11368, 2015

Impact of shipping emissions: scenarios for 2030

V. Matthias et al.

sen, D., Lee, D. S., Ng, S., Agrawal, A., Winebrake, J. J., Hoen, M., Chesworth, S., and Pandey, A.: Third IMO GHG Study 2014, Tech. rep., International Maritime Organization (IMO), London, UK, 2014. 11326, 11329

Steppeler, J., Doms, G., Schattler, U., Bitzer, H. W., Gassmann, A., Damrath, U., and Gregoric, G.: Meso-gamma scale forecasts using the nonhydrostatic model LM, Meteorol. Atmos. Phys., 82, 75–96, doi:10.1007/s00703-001-0592-9, 2003. 11333

Tiedtke, M.: A comprehensive mass flux scheme for cumulus parameterization in large-scale models, Mon. Weather Rev., 117, 1779–1800, doi:10.1175/1520-0493(1989)117<1779:ACMFSF>2.0.CO;2, 1989. 11333





ACPD

15, 11325–11368, 2015

ACPD
15, 11325–11368, 2015





**Table 1.** Number of days with 8 h maximum ozone concentrations greater than 120 µg m$^{-3}$ in 2030 in selected regions around the North Sea for the scenarios No ECA, ECA SCR 16, ECA SCR 21, and ECA opt.

| | 1 | 2 | 3 | 4 | 5 |
|---|---|---|---|---|---|
| 2011 | 9 | 19 | 27 | 46 | 29 |
| No ECA | 9 | 20 | 29 | 46 | 29 |
| ECA SCR 16 | 8 | 18 | 26 | 46 | 29 |
| ECA SCR 21 | 8 | 18 | 27 | 46 | 29 |
| ECA opt | 6 | 12 | 16 | 45 | 22 |

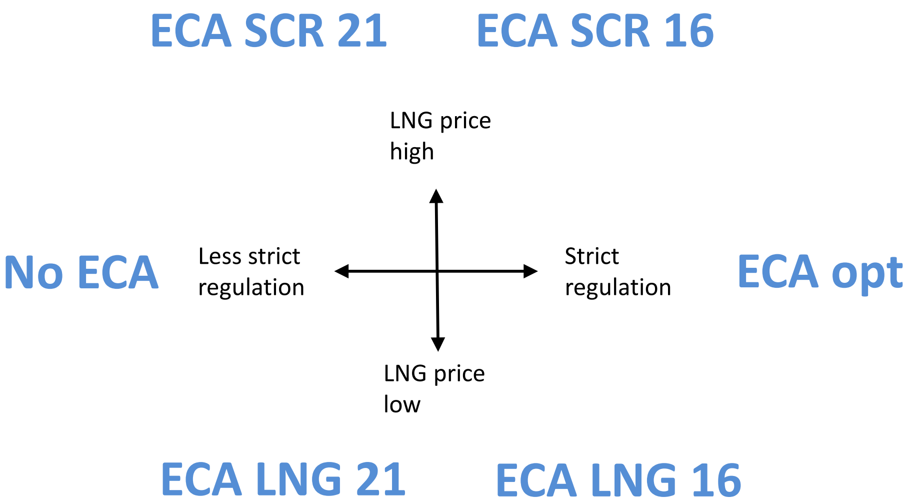


**Figure 1.** Scenario identifiers for technical developments and legislation with respect to ship emissions for 2030.





ACPD
15, 11325–11368, 2015
Impact of shipping emissions: scenarios for 2030
V. Matthias et al.

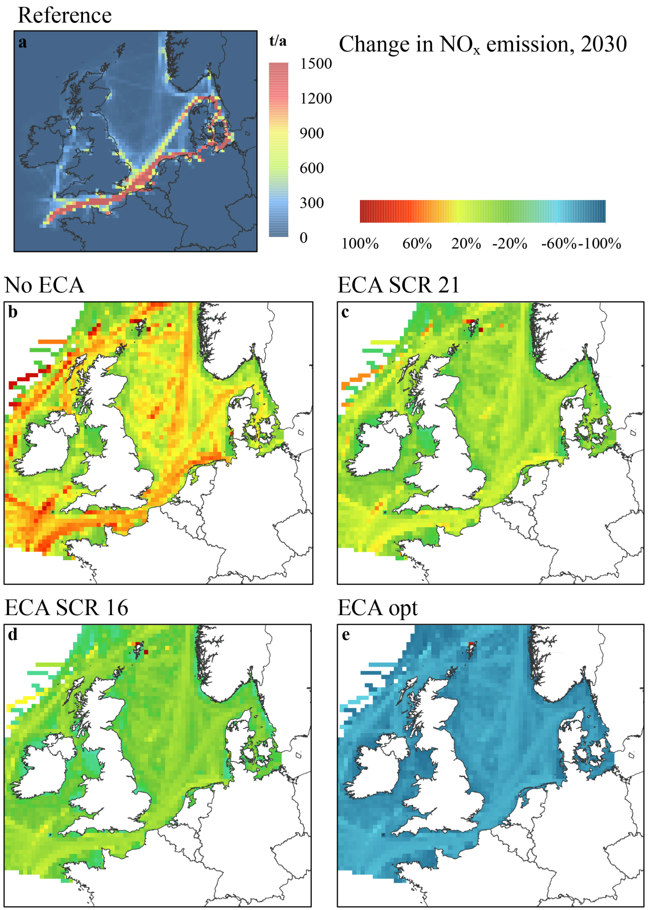


**Figure 2.** $NO_x$ emissions from ships, **(a)** annual totals in t per grid cell of 24 km × 24 km. Emission changes for the scenarios **(b)** No ECA, **(c)** ECA LNG, **(d)** ECA SCR, and **(e)** ECA opt for 2030.





ACPD
15, 11325–11368, 2015

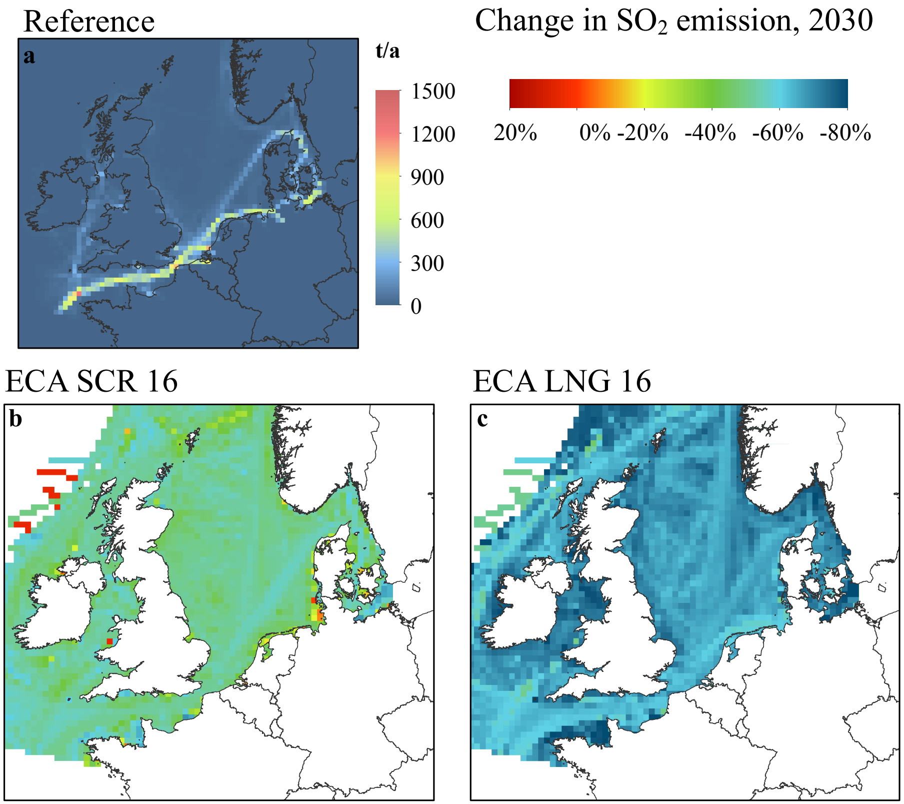


**Figure 3.** $SO_2$ emissions from ships, **(a)** annual totals in t per grid cell of 24 km × 24 km. Emission changes for the scenarios **(b)** ECA SCR 16, and **(c)** ECA LNG 16 for 2030.





ACPD
15, 11325–11368, 2015

Impact of shipping emissions: scenarios for 2030

V. Matthias et al.

Title Page
Abstract Introduction
Conclusions References
Tables Figures
◄ ►
Back Close
Full Screen / Esc
Printer-friendly Version
Interactive Discussion

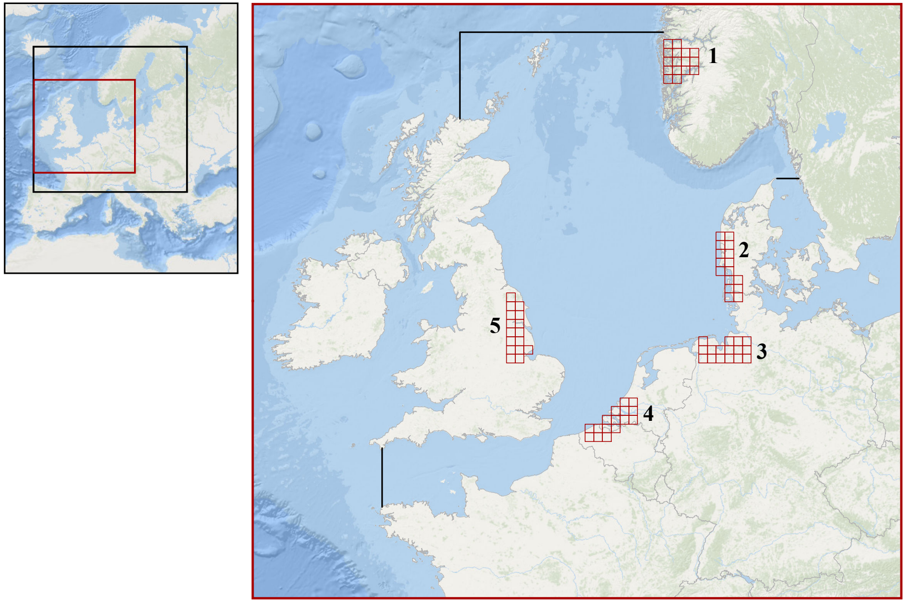


**Figure 4.** Left: modelling domains, outer domain with 72 km × 72 km resolution (outer black line), inner domain with 24 km × 24 km resolution (inner black line) and the evaluation area (red line). Right: evaluation area including the greater North Sea region illustrating also the five regions (namely 1 to 5) for which time series of pollutant concentrations have been derived from CMAQ modelling results.





ACPD
15, 11325–11368, 2015

Impact of shipping emissions: scenarios for 2030

V. Matthias et al.

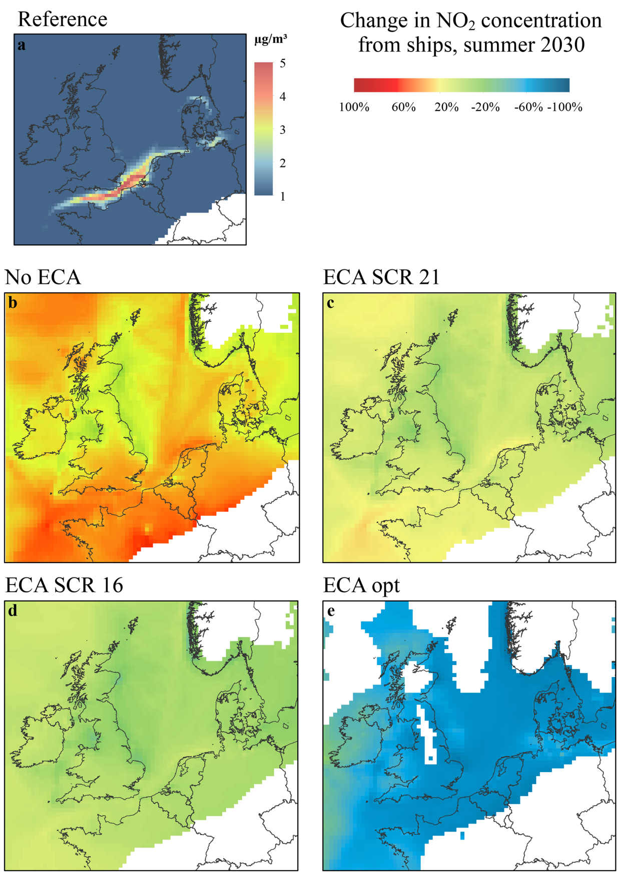


**Figure 5.** Contribution of shipping to the total $NO_2$ concentrations in summer (JJA) **(a)** today (Reference) and change in the scenarios **(b)** No ECA, **(c)** ECA SCR 21, **(d)** ECA SCR 16, **(e)** ECA opt.





ACPD
15, 11325–11368, 2015

Impact of shipping emissions: scenarios for 2030

V. Matthias et al.

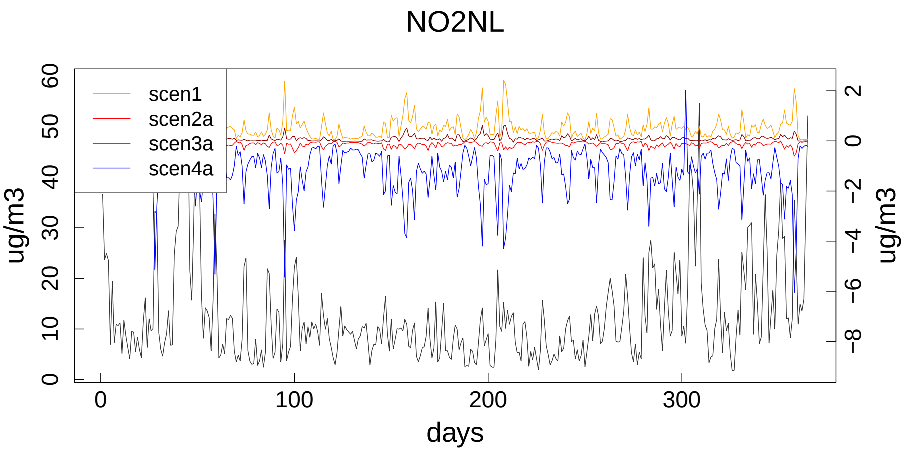


**Figure 6.** Time series of daily average $NO_2$ concentrations in $\mu g\,m^{-3}$ (black, left *y* axis) and the contribution of shipping to the $NO_2$ concentrations in the coastal areas of Belgium and the Netherlands (region 4) for all scenarios (colored, right *y* axis).





ACPD
15, 11325–11368, 2015

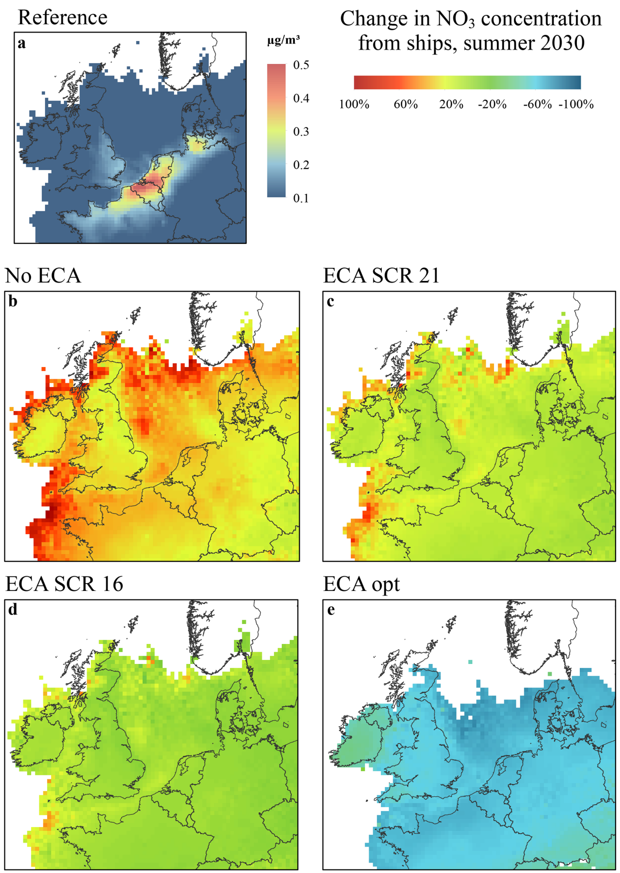


**Figure 7.** Contribution of shipping to the total $NO_3^-$ concentrations in summer (JJA) **(a)** today (Reference) and change in the scenarios **(b)** No ECA, **(c)** ECA SCR 21, **(d)** ECA SCR 16, **(e)** ECA opt.

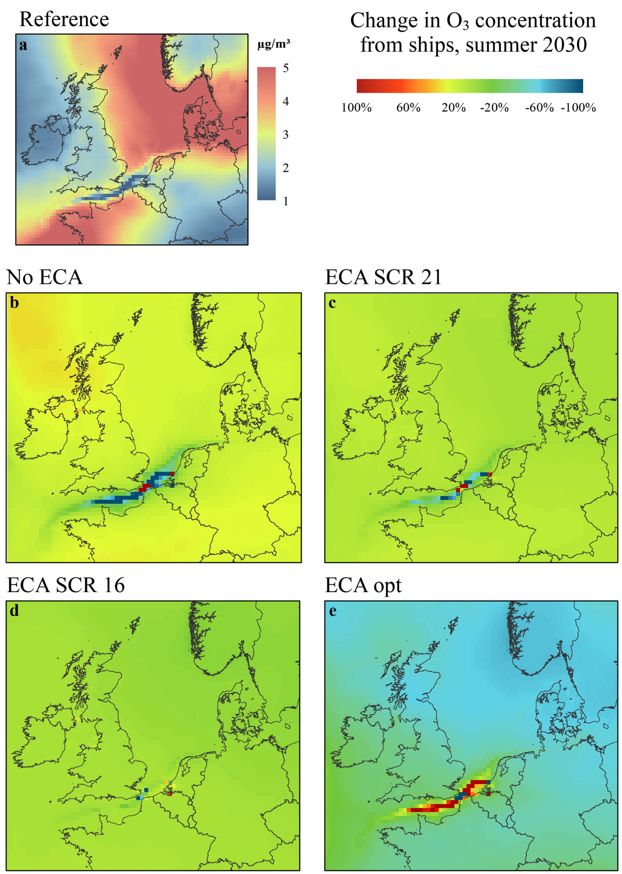


**Figure 8.** Contribution of shipping to the mean $O_3$ concentrations in summer (JJA) **(a)** today (Reference) and change in the scenarios **(b)** No ECA, **(c)** ECA SCR 21, **(d)** ECA SCR 16, **(e)** ECA opt.





ACPD
15, 11325–11368, 2015

Impact of shipping emissions: scenarios for 2030

V. Matthias et al.

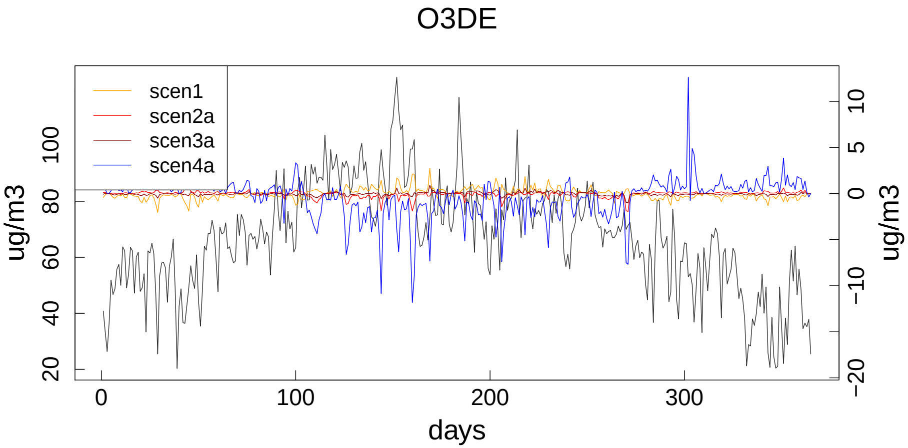


**Figure 9.** Time series of daily average ozone concentrations in μg m$^{-3}$ (shaded grey, left *y* axis) and the contribution of shipping to the ozone concentrations in the coastal areas of Germany (region 3) for all scenarios (right *y* axis). "noship" denotes the changes if all ship emissions were cut to zero





ACPD
15, 11325–11368, 2015

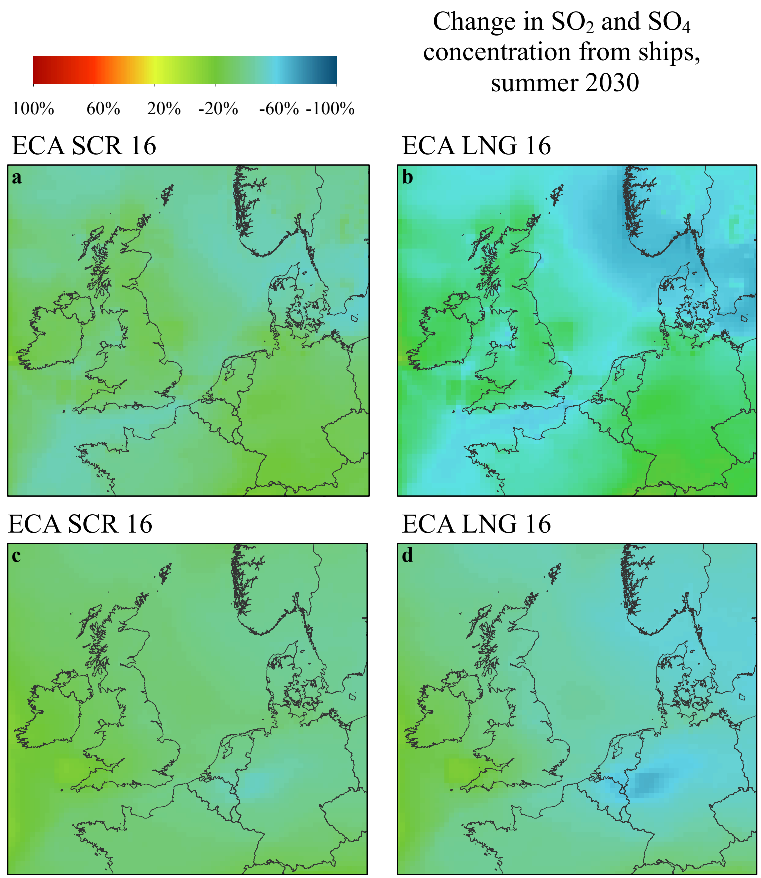


**Figure 10.** Change in the contribution of shipping to the total (**a** and **b**) $SO_2$ and (**c** and **d**) $SO_4$ concentrations in summer (JJA) for the scenarios ECA SCR 16 (left), ECA LNG 16 (right), in relation to the reference case. See Figs. A1 and A2 for the reference concentrations





ACPD
15, 11325–11368, 2015

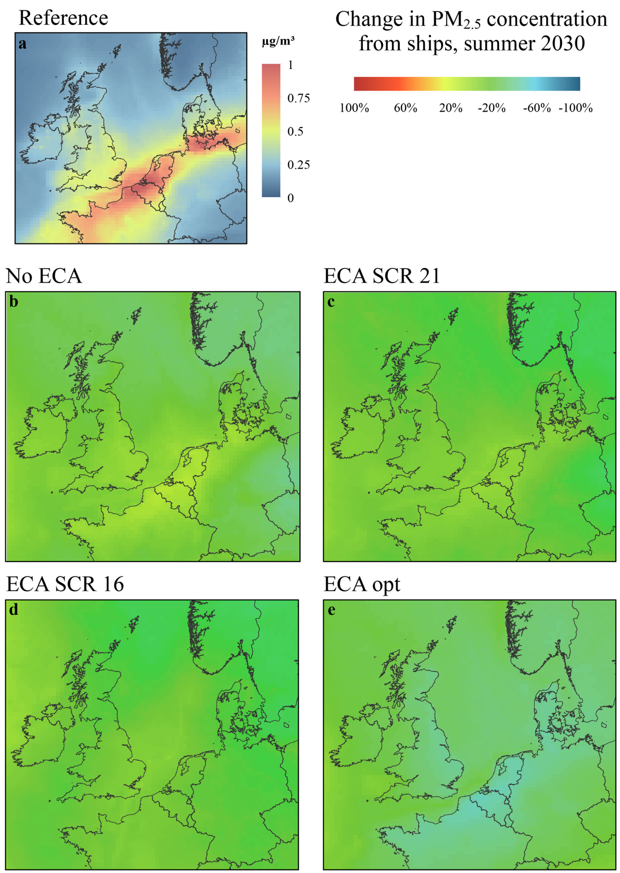


**Figure 11.** Contribution of shipping to the total $PM_{2.5}$ concentrations in summer (JJA) **(a)** today (Reference) and change in the scenarios **(b)** No ECA, **(c)** ECA SCR 21, **(d)** ECA SCR 16, **(e)** ECA opt.





ACPD
15, 11325–11368, 2015

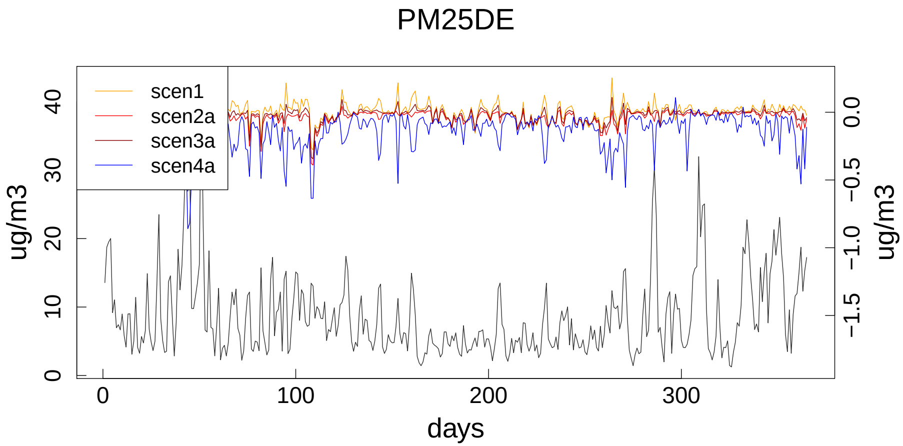


**Figure 12.** Time series of daily average $PM_{2.5}$ concentrations in $\mu g\,m^{-3}$ (black, left *y* axis) and the contribution of shipping to the $PM_{2.5}$ concentrations in the coastal areas of Germany (region 3) for the main scenarios (colored, right *y* axis).





ACPD
15, 11325–11368, 2015

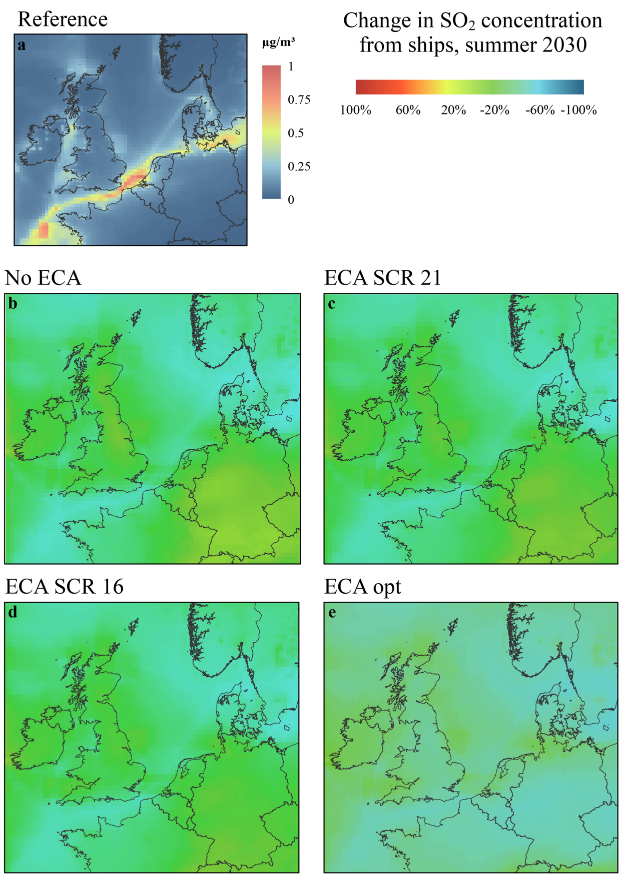


**Figure A1.** Change in the contribution of shipping to the total $SO_2$ concentrations in summer (JJA) compared to the reference case **(a)** for the scenarios **(b)** No ECA, **(c)** ECA SCR 16, **(d)** ECA SCR 21, and **(e)** ECA opt.





ACPD
15, 11325–11368, 2015

Impact of shipping emissions: scenarios for 2030

V. Matthias et al.

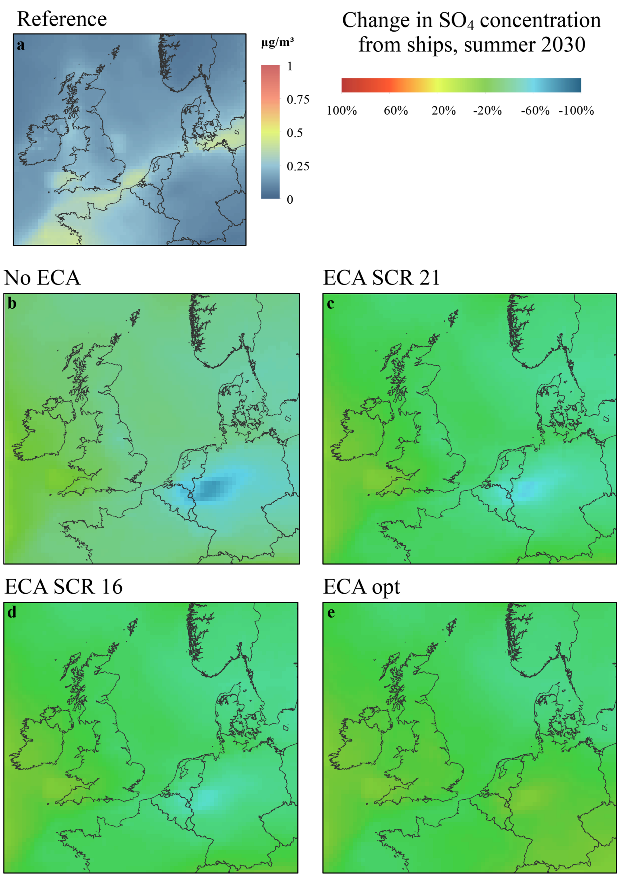


**Figure A2.** Change in the contribution of shipping to the total $SO_4$ concentrations in summer (JJA) compared to the reference case **(a)** for the scenarios **(b)** No ECA, **(c)** ECA SCR 16, **(d)** ECA SCR 21, and **(e)** ECA opt.





ACPD
15, 11325–11368, 2015

Impact of shipping emissions: scenarios for 2030

V. Matthias et al.

Title Page
Abstract Introduction
Conclusions References
Tables Figures
◀◀ ▶▶
◀ ▶
Back Close
Full Screen / Esc
Printer-friendly Version
Interactive Discussion

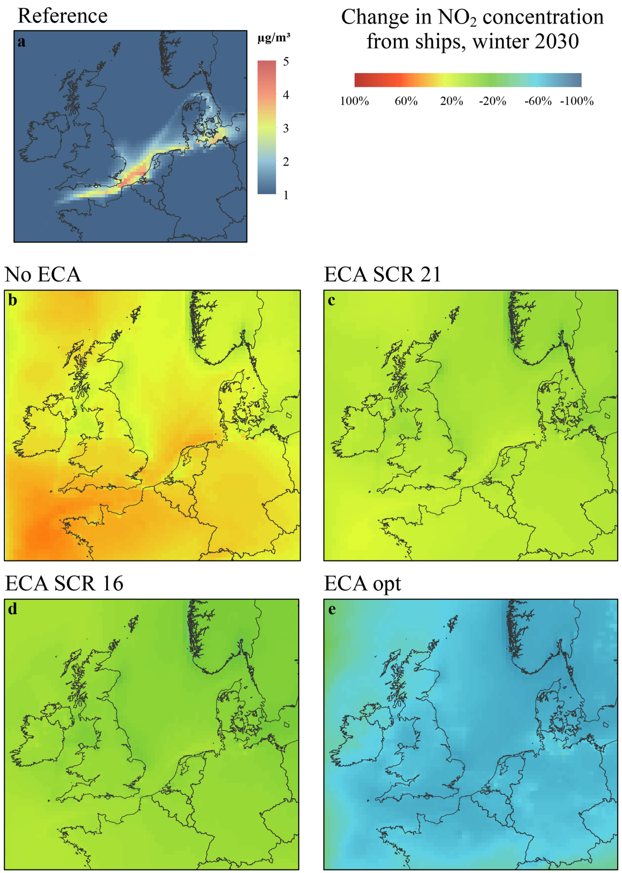


**Figure A3.** Change in the contribution of shipping to the total $NO_2$ concentrations in winter (DJF) compared to the reference case **(a)** for the scenarios **(b)** No ECA, **(c)** ECA SCR 16, **(d)** ECA SCR 21, and **(e)** ECA opt.





ACPD
15, 11325–11368, 2015

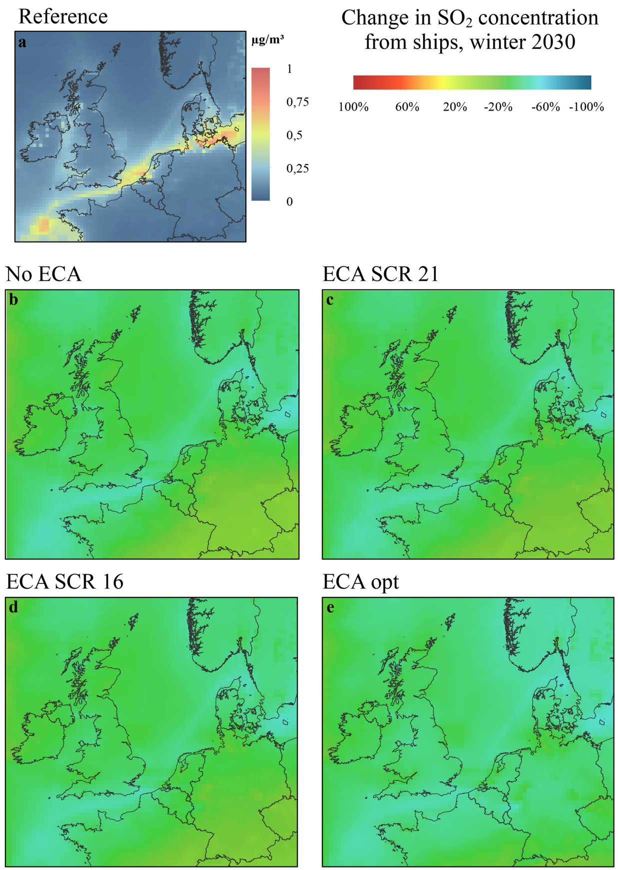


**Figure A4.** Change in the contribution of shipping to the total $SO_2$ concentrations in winter (DJF) compared to the reference case **(a)** for the scenarios **(b)** No ECA, **(c)** ECA SCR 16, **(d)** ECA SCR 21, and **(e)** ECA opt.



ACPD
15, 11325–11368, 2015

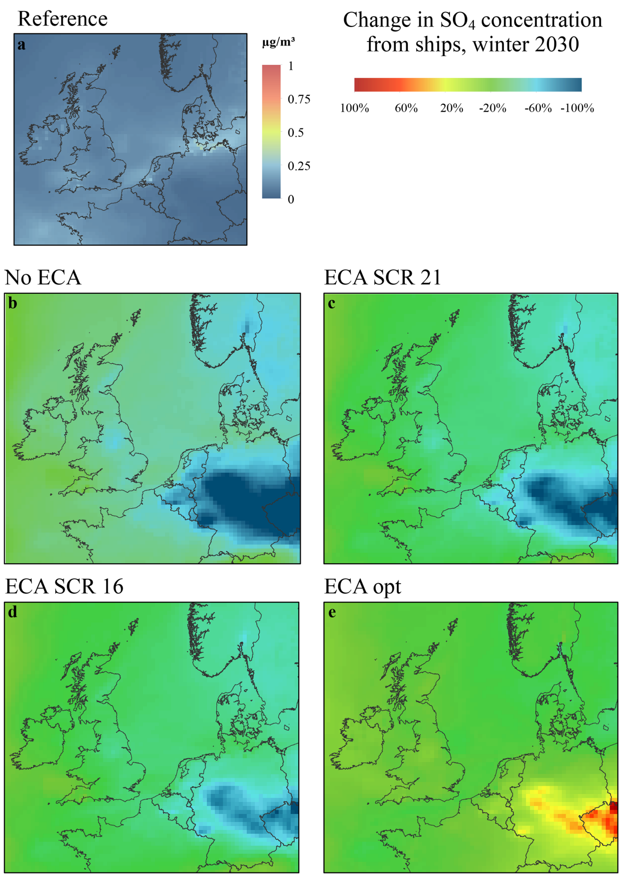


**Figure A5.** Change in the contribution of shipping to the total $SO_4$ concentrations in winter (DJF) compared to the reference case **(a)** for the scenarios **(b)** No ECA, **(c)** ECA SCR 16, **(d)** ECA SCR 21, and **(e)** ECA opt.





ACPD
15, 11325–11368, 2015

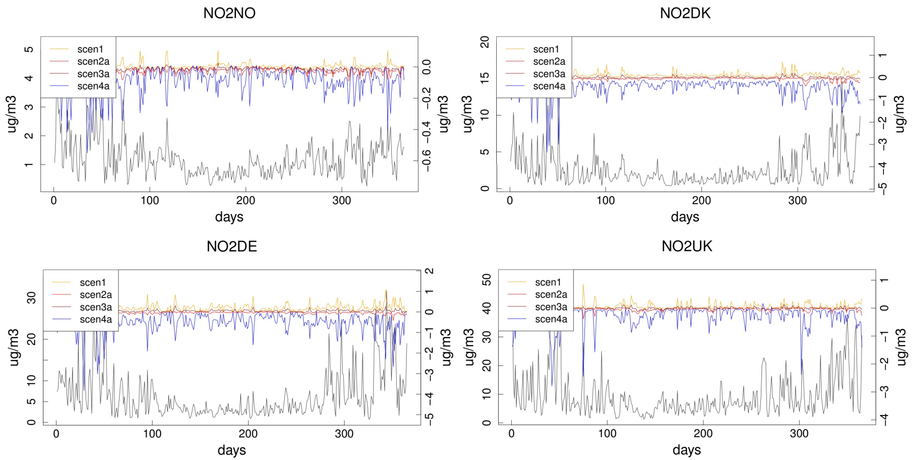


**Figure A6.** Time series of daily average $NO_2$ concentrations in $\mu g\,m^{-3}$ (black, left $y$ axis) and the contribution of shipping to the $NO_2$ concentrations in the coastal areas of Norway (region 1), Denmark (region 2), Germany (region 3), and Great Britain (region 5) for all scenarios (right $y$ axis).





ACPD
15, 11325–11368, 2015

Impact of shipping emissions: scenarios for 2030

V. Matthias et al.

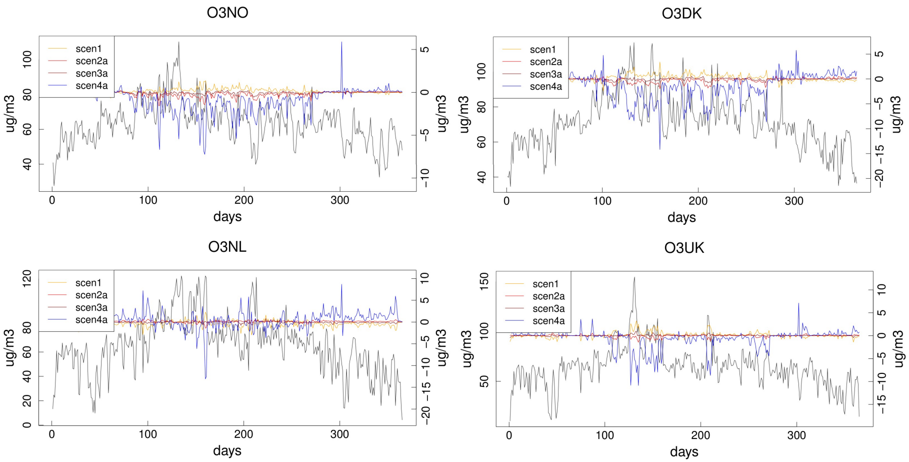


**Figure A7.** Time series of daily average $O_3$ concentrations in $\mu g\,m^{-3}$ (black, left *y* axis) and the contribution of shipping to the $O_3$ concentrations in the coastal areas of Norway (region 1), Denmark (region 2), Belgium and the Netherlands (region 4), and Great Britain (region 5) for all scenarios (right *y* axis).





ACPD
15, 11325–11368, 2015

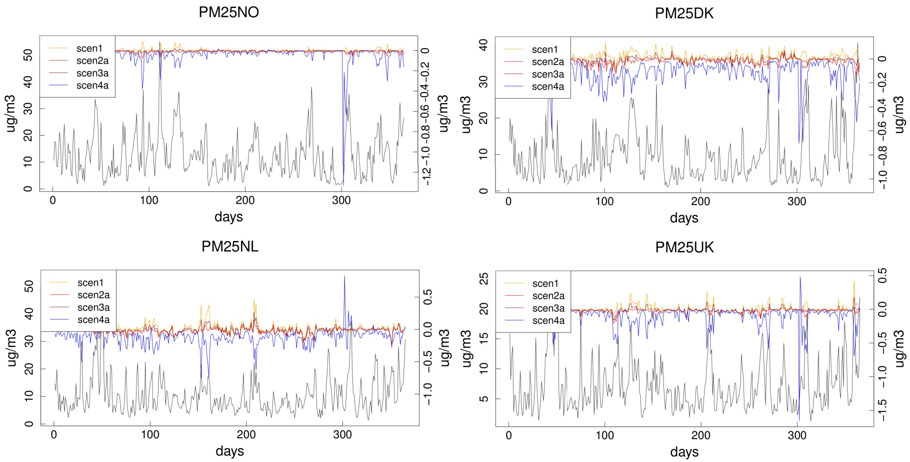


**Figure A8.** Time series of daily average $PM_{2.5}$ concentrations in $\mu g\,m^{-3}$ (black, left $y$ axis) and the contribution of shipping to the $PM_{2.5}$ concentrations in the coastal areas of Norway (region 1), Denmark (region 2), Belgium and the Netherlands (region 4), and Great Britain (region 5) for all scenarios (right $y$ axis).





ACPD
15, 11325–11368, 2015